CICE2023 Rio de Janeiro – Brazil 11TH INTERNATIONAL CONFERENCE ON FRP COMPOSITES IN CIVIL ENGINEERING

EVALUATION OF FRP-REINFORCED CONCRETE MEMBERS WITHOUT SHEAR REINFORCEMENT – ANALYSIS USING SHEAR CRACK PROPAGATION THEORY (SCPT)

Morvarid Fattahi, University of Ottawa, Ottawa, Canada, mfatt100@uottawa.ca
Maximilian Schmidt, RWTH Aachen University, Aachen, Germany, mschmidt@imb.rwth-aachen.de
Sven Bosbach, RWTH Aachen University, Aachen, Germany, sbosbach@imb.rwth-aachen.de
Martin Noël, University of Ottawa, Ottawa, Canada, MartinNoel@uottawa.ca
Josef Hegger, RWTH Aachen University, Aachen, Germany, jhegger@imb.rwth-aachen.de
Martin Classen, RWTH Aachen University, Aachen, Germany, mclassen@imb.rwth-aachen.de

ABSTRACT
The determination of the maximum shear capacity of reinforced concrete (RC)-beams and slabs has been a challenging task for more than 100 years. To gain deeper insights into the shear capacity of RC members and to search for a mechanical solution to determine the ultimate capacity and to explain the phenomen of one-way shear, the so-called Shear Crack Propagation Theory (SCPT) has been developed. The proposed theory is not limited to steel RC members and can be applied to members with non-metallic reinforcement accounting for their material parameters and constitutive relationships. Further, the SCPT does not focus only on the ultimate state but also on the behaviour during the loading process up to failure. In this publication, the application of the SCPT to RC-members with longitudinal FRP-reinforcement without stirrups is presented.

KEYWORDS
Shear strength; SCPT; Shear Crack Propagation Theory; Fiber-reinforced polymers; Crack propagation

INTRODUCTION
One of the challenging issues which has attracted continuous attention in the last century is the shear behavior of reinforced concrete (Kani, 1964; Reineck, 1991; Yoo, 2022). Interaction of several parameters such as the geometrical properties including shear slenderness, load distribution, concrete properties, strength and details of shear reinforcement, and the ratio of tensile and shear reinforcement result in a higher degree of complexity than flexural behavior (Adam et al., 2022; Huber et al., 2016; Wu & Hu, 2017). Furthermore, the prediction of failure regions and their ultimate strength is also complicated because one-way shear failure of reinforced concrete beams occurs through several simultaneous damage mechanisms that include diagonal cracks, crushing of concrete struts, bond failure between main reinforcement and concrete, and failure and yielding of shear reinforcement (Rombach et al., 2011).

In the past, engineers mainly relied on empirical approaches to predict shear strength of RC members, for which a correspondingly large safety factor must be taken into account in order to achieve a specified reliability of structural members. For an economical at one hand and safe design at the other hand, this has led to increased research efforts to understand the "mechanical behavior" of shear transfer actions in diagonally cracked members. Recently, a new mechanics-based approach known as the “Shear Crack Propagation Theory” (SCPT) was developed that combines concepts of crack kinematics with constitutive material models to predict shear crack behavior at all stages of loading up to failure in reinforced concrete (RC) members. Development of the SCPT (Classen, 2020) culminated years of research examining the effects of crack localization, cantilever action, shear in compression zone, aggregate interlock, dowel action, and crack bridging action to arrive at a unified approach to predict the shear behavior of RC beams and slabs without shear reinforcement. The SCPT allows for predictions of shear crack geometry, transferred shear (including contributions of all shear transfer actions), as well

as corresponding strains and deformations over the entire loading process from crack initiation up to the point of shear failure.

In RC beams, the shear force is initially primarily resisted by the compression zone of intact concrete. This zone can fail through compression crushing or tensile cracking due to combined compressive and shear stresses. Slender beams experience failure through inclined tensile cracking (Choi et al., 2007). The fracture process zone refers to the area where microcracks grow in a material, and it can be modelled using a cohesive behavior. Concrete transfers stresses across cracks until a maximum crack width is reached, and beyond this width, the cohesive behavior disappears due to increased shear and bending. Aggregate interlock refers to the occurrence of cracks between aggregates and the cement paste in concrete. Longitudinal reinforcement is employed to lock these two sides of the crack together. Various factors such as aggregate properties, cement paste characteristics, crack unevenness, and size can influence the effectiveness of aggregate interlock. The activation of this phenomenon, triggered by the sliding of cracked lips, directly influences the shear behavior of the concrete. In addition, the dowelling action of reinforcement occurs when the number of cracks in concrete exceeds a certain threshold. It is influenced by factors such as the bending stiffness of longitudinal reinforcement and the concrete cover. However, the effectiveness of this action is limited by the concrete's tensile strength. The dowelling action does not generate additional forces in the shear crack and can even hinder a secondary crack propagation process at the tip of the shear crack. (Classen, 2020).

To date, the SCPT has only been applied to steel-RC members, although there is no inherent limitation in the model to any particular reinforcement type provided that appropriate constitutive models are adopted. Although steel remains the most common reinforcing material for concrete structures due to its favorable mechanical properties and competitive cost, the use of fiber-reinforced polymer (FRP) reinforcing bars continues to increase around the world as a corrosion-resistant alternative, particularly in marine environments and where de-icing salts are used. The mechanical properties of FRP reinforcement differ from steel in several ways that can influence shear behavior of RC beams. The relatively lower modulus of elasticity of FRP means that, for the same reinforcement ratio, wider and deeper cracks will develop compared to steel-RC members, reducing shear transfer associated with aggregate interlock and the depth of the uncracked compression zone. Similar effects also influence the contribution of dowel action and tension stiffening.

Due to its mechanical basis, the SCPT is well-suited to investigate the contributions of various shear transfer mechanisms and develop a deeper understanding of the effects of reinforcement type on overall shear behavior of RC beams. This research presents a preliminary study extending the application of SCPT to FRP-RC members.

METHODOLOGY

Details of the SCPT procedure are reported by Classen (2020). Figure 1 shows the general incremental procedure to evaluate the shear strength of RC members at a particular location of the beam (defined as $d \cdot \lambda_{cs}$ from the support). Figure 1-b shows the shear force-deformation history of four states of the shear crack propagation which are elaborated in Figure 1-c. For a given neutral axis depth (x_0), the model determines the location of the crack tip (x_1) from the center of rotation (CR) that satisfies conditions of equilibrium and compatibility. The CR can change during the loading process, and x_1 can be positive when shear crack is in the tensile zone and negative when the shear crack is in the compression zone (Fig. 2). The shear transfer mechanism after concrete cracking depends both on kinematic behavior (i.e., crack deformations, steel and concrete strains) and constitutive behavior (including fracture process zone (FPZ), aggregate interlock, and dowel action of reinforcement as shown in Fig. 3) (Classen, 2020).

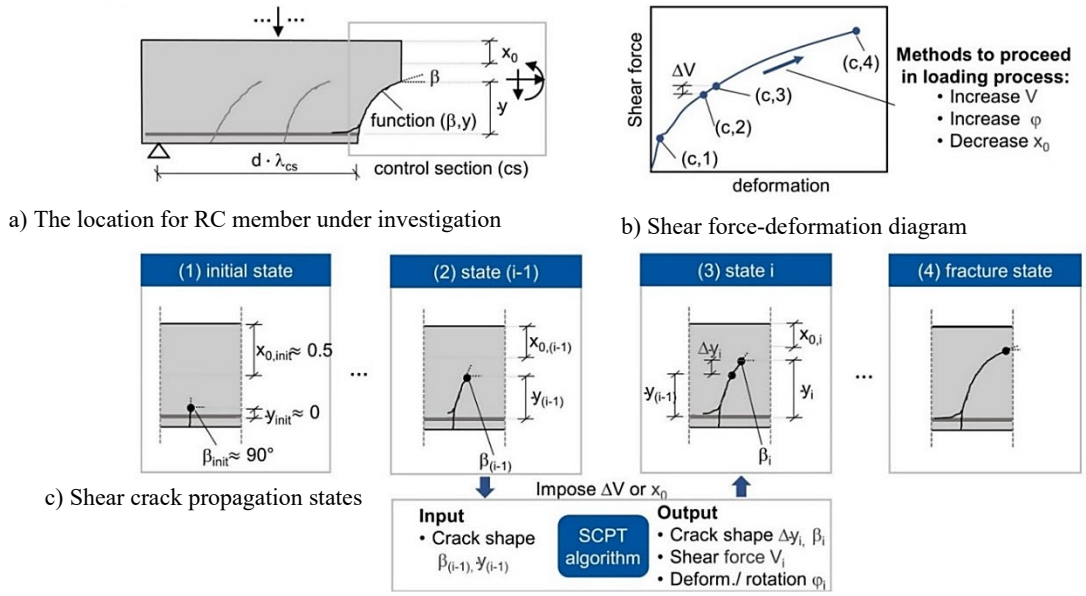

a) The location for RC member under investigation

b) Shear force-deformation diagram

c) Shear crack propagation states

d) SCPT algorithm

Figure 1: Procedure of shear crack propagation (reproduced from Classen, 2020)

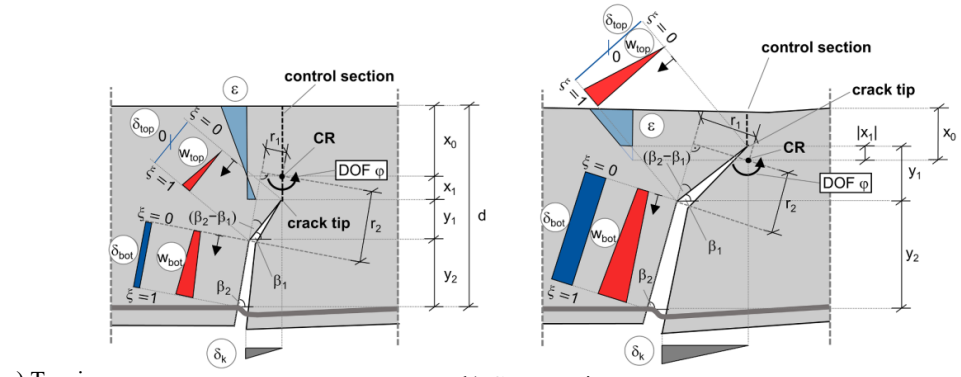

a) Tension zone

b) Compression zone

Figure 2: Kinematic model for two different crack opening zones (tension and compression zone) (reproduced from Classen, 2020)

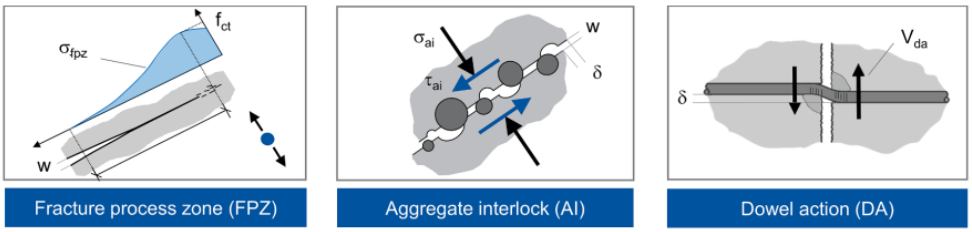

Figure 3: Process of shear transfer action among the shear cracks (reproduced from Classen, 2020).

The SCPT algorithm employs an iterative strategy based on some initial assumptions. All the geometrical data, material properties, loading conditions, and the geometry of the previous shear crack in step (i-1) are supposed as input data. Then, the transferred shear stress above the crack tip (τ_0) and the concomitant horizontal crack tip stress (σ_{x0}) will be calculated by estimating the crack propagation angle and length (β_{estim}, Δy_{estim}), the vertical crack tip stress ($\sigma_{z0,estim}$), and the expected rotation angle of the shear crack (φ_{estim}). After that, the crack opening (w), crack sliding (δ), and the distance between the crack tip and center of rotation (x_1) should be determined (Classen, 2020).

In the next step, normal and shear forces in the continuous uncracked concrete, and shear transfer action along the crack is calculated. The total transferred shear force (V_E), bending moment (M_E) in the control

section, and the corresponding tensile force in the reinforcement (F_s) will be obtained to satisfy equilibrium conditions. Then, the rotation of the shear crack (φ_{calc}), vertical crack tip stress ($\sigma_{z0,calc}$), shear transfer action in the crack, corresponding tensile force in reinforcement, crack propagation angle, and the concomitant vertical crack extension are calculated. At this step, the validity of the initial assumptions are assessed. If it is valid, it means that a compatible state of equilibrium and crack propagation is discovered. Otherwise, other initial assumptions should be considered. Finally, it is worth mentioning that the output of the SCPT are β and y (crack geometry), φ rotation of the control section (deformations), and all internal forces (Classen, 2020).

In this study, a preliminary parametric analysis is presented that investigates the use of the SCPT for FRP-RC beams. The analysis is based on a reference steel-RC beam (320 mm wide x 350 height, shear span-to-depth ratio of 4.33, containing five 16 mm diameter steel reinforcing bars, and maximum aggregate size of 16 mm) previously tested and analysed by Schmidt et al. (2021) and modified in three steps to account for the different mechanical properties of FRP reinforcement:

Step 1: the Young's modulus of the reinforcement is changed from E_s = 200 GPa (steel) to E_f = 50, 100, and 150 GPa representing a range of FRP materials;

Step 2: the reduced dowel action associated with FRP reinforcement is introduced according to the results of previous studies. Although the transverse shear strength of FRP reinforcing bars is considerably lower than steel bars of the same diameter, dowel action is still largely controlled by the splitting strength of the concrete cover. Unfortunately, there is no consensus regarding this effect, with some researchers suggesting that the effect of bar stiffness can be neglected (e.g., Oller, 2015), while others have reported a significant influence. Tottori and Wakui (1993) suggested that the dowel capacity of test specimens reinforced with FRP bars is about 70% of those containing reinforcing steel with the same diameter, corresponding to $(Ef/Es)^{1/3}$. Michaluk et al. (1998) claimed that the effect is directly proportional to elastic modulus and proposed to modify existing equations by the modular ratio of the reinforcement (Ef/Es). As previous research is not conclusive, the dowel action is modified in this study by the factor $(Ef/Es)^{1/3}$; this can be easily adapted in future works as more detailed studies emerge on this topic.

The modified formulations, based on the work of Reineck (1990) and Yang (2014) adopted by Classen (2020), are given by Equations 1 to 3:

$$V_{da,0} = 1.64 \cdot b_n \cdot \phi_s \cdot f_c^{1/3} \left(\frac{E_f}{E_s}\right)^{1/3} \quad \text{Eq. 1}$$

$$b_n = b_w - \phi_s \cdot n_s \quad \text{Eq. 2}$$

$$V_{da} = \begin{cases} \delta_k \leq 0.05mm: & V_{da,0} \cdot \frac{\delta_k}{0.05} \cdot \left(2 - \frac{\delta_k}{0.05}\right) \\ \delta_k > 0.05mm: & V_{da,0} \cdot \frac{2.55 - \delta_k}{2.5} \geq 0 \end{cases} \quad \text{Eq. 3}$$

Where $V_{da,0}$ is the shear contribution of dowel action, b_n is the concrete net width activated in tension, b_w is the beam width, ϕ_s is the maximum aggregate size, f_c is the concrete compressive strength, E_f is FRP modulus of elasticity, E_s is reinforcement modulus of elasticity, n_s is the number of reinforcement, and δ_k is the vertical shear deformation at the level of flexural reinforcement.

Step 3: the effect of tension stiffening on shear capacity (Figure 4) is frequently neglected for steel-RC members. However, Bischoff and Paixao (2004) demonstrated that tension stiffening is more significant in FRP-RC due to the lower elastic modulus of the

reinforcement which makes the contribution of the concrete in tension proportionally larger. They proposed to normalize the post-cracking reinforcement strain by the modular ratio of the reinforcement (Ef/Es) in tension stiffening formulations to account for this difference.

Thus, it is proposed to modify the tension stiffening model developed by Bentz (2005) and adopted in Classen (2020) to give Equations 4 to 7:

$$\sigma_s(\varepsilon_{s,ts}) = \frac{F_s}{A_s} = \varepsilon_{s,ts} \cdot E_s + \frac{f_{ct}}{1+\sqrt{3.6 \cdot M \cdot \varepsilon_{s,ts} \cdot (\frac{E_f}{E_s})}} \quad \text{Eq. 4}$$

$$M = \frac{A_{c,eff}}{\sum d_s \cdot \pi} \quad \text{Eq. 5}$$

$$A_{c,eff} = h_{c,eff} \cdot b_w \quad \text{Eq. 6}$$

$$h_{c,eff} = min\left(2.5 \cdot d_1; \frac{h-x_0}{3}\right) \quad \text{Eq. 7}$$

Where F_s is the tensile force in the flexural reinforcement, A_s is reinforcement area, $\varepsilon_{s,ts}$ is the reinforcement strain in the region where bond is intact, f_{ct} is the concrete uniaxial tensile stress, M is bond parameter, $A_{c,eff}$ is area of the concrete effectively bonded to the bar, d_s is reinforcement diameter in concrete stiffened area, d_1 is concrete cover, h is the beam height, and x_0 is the imposed compression zone depth.

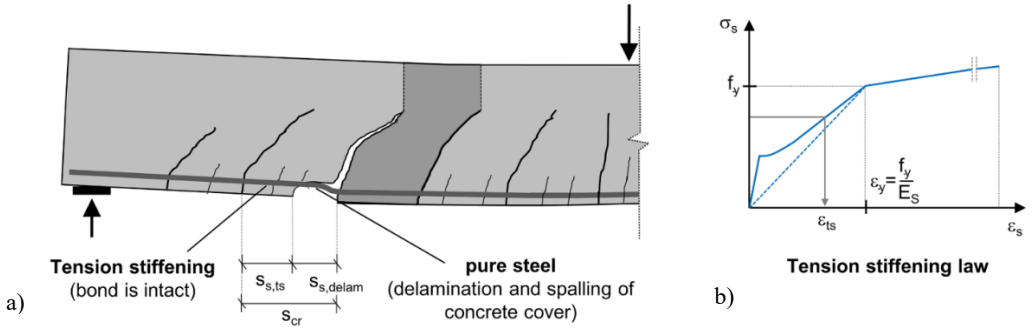

Figure 4: a) Tension stiffening region, b) tension stiffening law (reproduced from Classen, 2020).

The constitutive models used in this study follow the approach reported in greater detail in Classen (2020) and Schmidt et al (2021).

RESULTS

A detailed validation of the SCPT with experimental test results from a steel-RC beam is presented by Schmidt et al. (2021) (Figure 5). Four primary mechanisms are discussed here to evaluate the results of this analysis:

- Shear in the uncracked zone (V_{uncr});
- Shear in the fracture process zone (V_{FPZ});
- Shear transfer by aggregate interlock, activated once the crack propagation starts to become curved and results from sliding deformation of the crack (V_{ai});
- Shear transfer associated with dowel action, activated just after the inclined bending crack forms (V_{da}).

Figure 6 presents the shear force vs. crack rotation for RC beams having the same geometry and reinforcement as that from Schmidt et al. (2021), except with different values of elastic modulus of the reinforcement. The shear capacity corresponding to elastic moduli of 50, 100, 150, and 200 GPa were

47.5, 109.3, 158.2, and 167.7 kN, respectively (Table 1). Decreasing the modulus of elasticity from 200 GPa to 150 GPa reduced the ultimate strength by only 6%, whereas reinforcement with an elastic modulus of 50 GPa exhibited a shear capacity that was 72% lower than the reference beam.

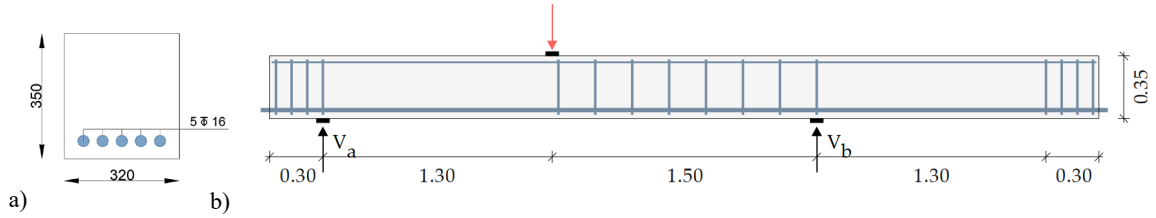

Figure 5: a) Section beam geometry (mm), b) Side view of beam (m) (Schmidt et al., 2021).

Table 1: The absolute values of various components at shear failure for different moduli of elasticity (kN)

V_{uncr}	V_{FPZ}	V_{ai}	V_{da}	Total V
E = 50 GPa				
22.83	3.74	0	20.92	47.49
E = 100 GPa				
25.54	10.17	54.19	19.36	109.26
E = 150 GPa				
27.46	11.37	101.45	17.96	158.24
E = 200 GPa				
31.43	13.58	104.43	18.30	167.74

For reinforcement moduli between 100 and 200 GPa, the contribution of dowel action remained constant at about 20 kN beyond a certain shear crack rotation angle (between 1.0 to 1.5 mrad), which also corresponded to the point where aggregate interlock began to increase. However, for the lowest value of modulus of elasticity (E=50 GPa), dowel action contribution was still increasing beyond 2 mrad rotation, and aggregate interlock did not contribute to shear capacity. In general, the combined contribution of dowel action, uncracked zone, and fracture process zone were relatively unaffected by changes in the elastic modulus, whereas a significant effect on aggregate interlock was observed which is attributed to the effect of reinforcement stiffness on limiting the width of shear cracks.

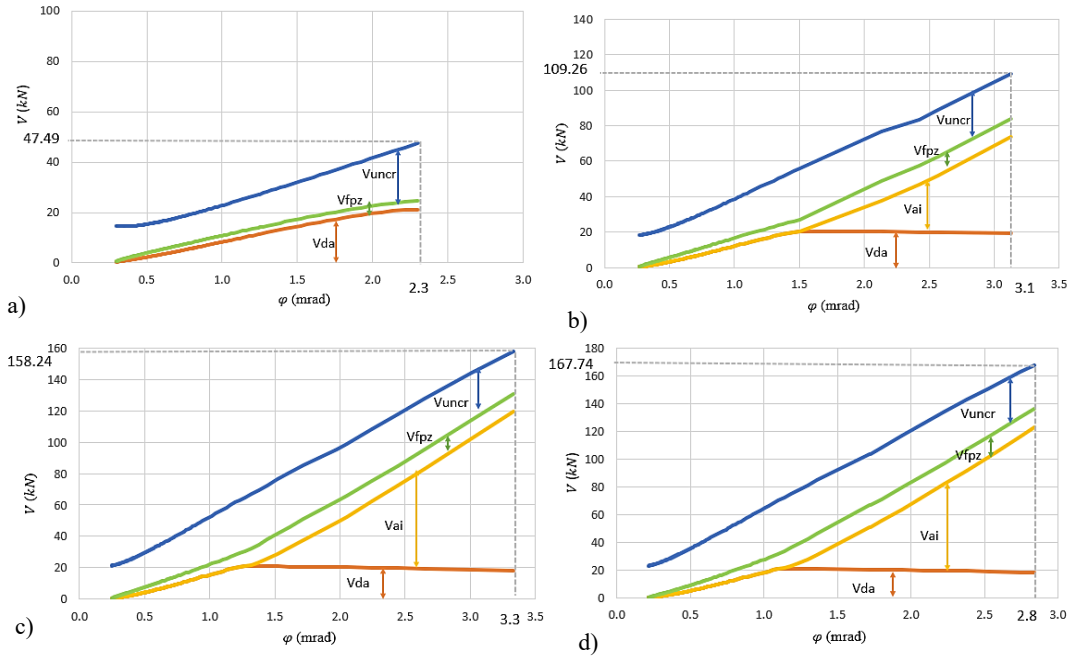

Figure 6: The relationship between shear force and crack rotation for various moduli of elasticity: a) E = 50 GPa, b) E = 100 GPa, c) E = 150 GPa, and d) E = 200 GPa.

Figure 7 presents the contribution of each mechanism in relative terms. In the early stages of loading, almost all of the shear force is carried by the uncracked concrete; although the value of V_{uncr} remains relatively constant throughout the test, its relative contribution decreases rapidly as the crack rotation increases. At failure, the contribution of the uncracked zone was approximately 50% for the low modulus reinforcement (50 GPa) but only about 20% for reinforcement with moduli between 100 to 200 GPa (Table 2). The shear transferred through the fracture process zone remained relatively stable at approximately 10% of the total shear force regardless of the reinforcement stiffness.

The contribution of dowel action and aggregate interlock were related; dowel action was more dominant at lower values of crack rotation (i.e., lower angle of inclination), reaching a peak value between 30 to 50% of the total shear force before gradually decreasing to a value between 10 to 50% at the failure load. The peak value for dowel action coincided with the aggregate interlock mechanism engaging in resisting shear, which quickly increased to become the dominant mechanism (50 to 60% of total shear) for beams with reinforcement stiffness between 100 and 200 GPa. Conversely, aggregate interlock did not play a role in the shear resistance of the beam with low reinforcement stiffness (50 GPa).

Table 2: The percentage of various components at shear failure for different moduli of elasticity (%)

V_{uncr}	V_{FPZ}	V_{ai}	V_{da}	Total V
E = 50 GPa				
48.2	9.4	0	42.4	100
E = 100 GPa				
21.8	8.6	53.0	16.6	100
E = 150 GPa				
17.4	7.2	64.0	11.4	100
E = 200 GPa				
16.8	7.6	65.4	10.2	100

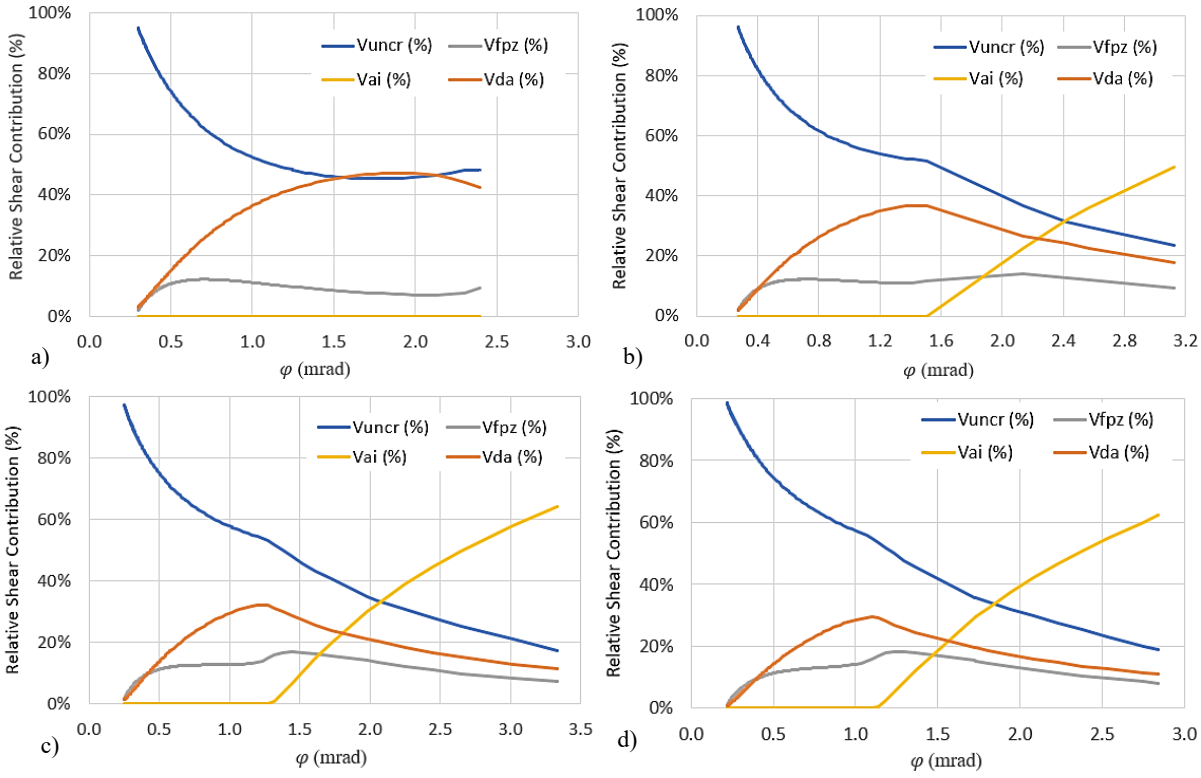

Figure 7: The relative shear contribution and crack rotation for various moduli of elasticity: a) E = 50 GPa, b) E = 100 GPa, c) E = 150 GPa, and d) E = 200 GPa.

In step 2, the dowel action was modified by the ratio $(Ef/Es)^{1/3}$, keeping all other parameters constant, giving the results presented in Figure 8. The total shear resistance was reduced by 2.3%, 4.6%, and 8.9% for beams with reinforcement elastic moduli of 50, 100, and 150 GPa, respectively (Table 3). The slight reduction in dowel action reduced the crack rotation at failure as well as the rotation angle at which aggregate interlock was engaged. Even the beam containing 50 GPa reinforcement exhibited a small contribution from aggregate interlock at failure (Table 4).

Table 3: The absolute values of various components at shear failure for different moduli of elasticiy (kN)

V_{uncr}	V_{FPZ}	V_{ai}	V_{da}	Total V
E = 50 GPa				
22.71	7.07	3.61	13.02	46.41
E = 100 GPa				
24.19	10.65	53.92	15.51	104.27
E = 150 GPa				
30.05	12.03	85.05	16.94	144.07

Table 4: The percentage of various components at shear failure for different modulus of elasticities (%)

V_{uncr}	V_{FPZ}	V_{ai}	V_{da}	Total V
E = 50 GPa				
48.9	15.2	7.8	28.1	100
E = 100 GPa				
23.2	10.2	51.7	14.9	100
E = 150 GPa				
20.9	8.3	59.0	11.8	100

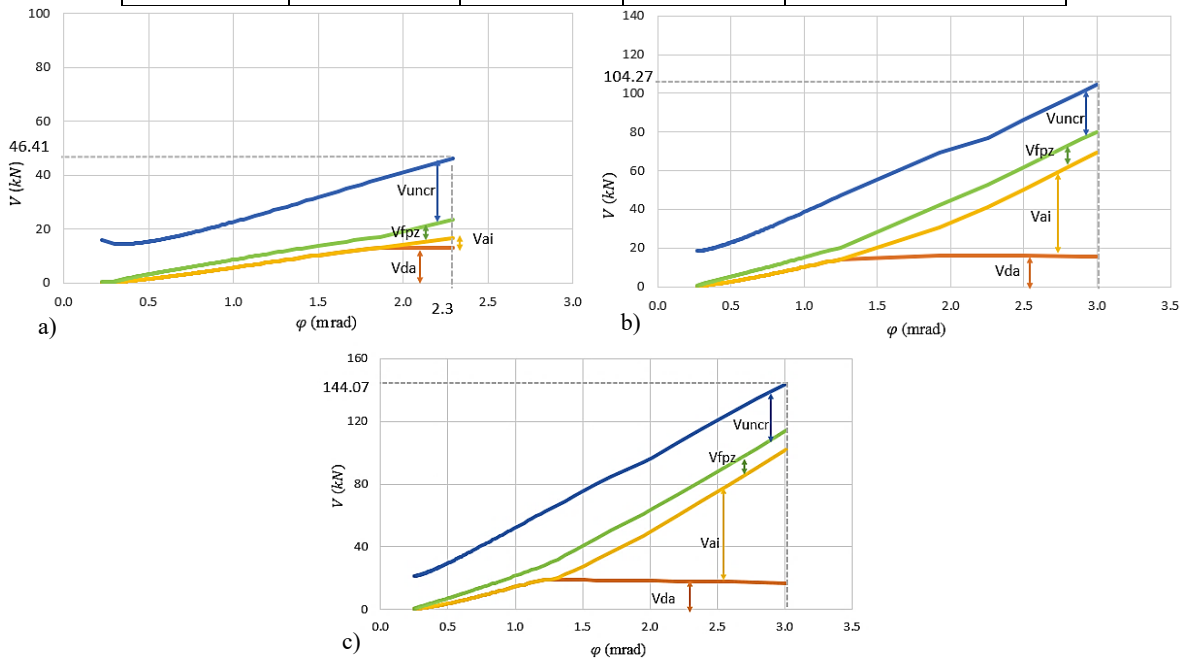

Figure 8: The relationship between shear force and crack rotation for various moduli of elasticity with reduced dowel action: a) E = 50 GPa, b) E = 100 GPa, and c) E = 150 GPa.

The effect of tension stiffening on the shear behavior of FRP-RC beams is currently under investigation. Verification of model results with experimental data will be carried out in the next stage of this research.

CONCLUSIONS

In this research, the SCPT method has been briefly summarized and extended to the beams reinforced with FRP bars, which are increasingly used as a corrosion-resistant alternative to steel reinforcement to design longer lasting structures. The use of FRP reinforcement is known to significantly influence shear behavior of RC beams because of their lower elastic moduli, dowel capacity, and different bond characteristics compared to steel bars.

The SCPT allows the contributions of different shear transfer mechanisms to be evaluated at all stages of loading. Based on the results of this study, the following preliminary conclusions can be drawn:

- The shear force carried by the uncracked concrete in the compression zone remains relatively constant throughout the loading process, and is not significantly affected by reinforcement stiffness. The relative contribution to total shear resistance decreases as contributions from other mechanisms increase with increasing crack rotation. At failure, the contribution of the uncracked zone ranged from approximately 20% of the total shear force for beams with reinforcement having Young's moduli of 100, 150, and 200 GPa, to approximately 50% for 50 GPa reinforcement.
- The shear force transferred through the fracture process zone remained relatively stable between 10-20% of the total shear force throughout most of the loading process up to failure, and was not significantly affected by the reinforcement stiffness.
- Dowel action increased gradually before reaching a constant value, typically at crack rotation values between approximately 1-2 mrad. The relative contribution of dowel action to total shear force peaked at around 30-50% before decreasing to 10-40% at failure. Decreasing the dowel action to account for the lower transverse shear strength of the reinforcement resulted in slight overall decreases in shear capacity from about 2 to 9% for beams with reinforcement moduli between 50 to 150 GPa.
- Aggregate interlock began to participate in shear transfer once the dowel force reached its peak value. For low stiffness reinforcement (50 GPa), the contribution of aggregate interlock was small or negligible, while for reinforcement stiffness between 100 to 200 GPa, this shear transfer mechanism was dominant at failure corresponding to 50 to 60% of the total shear force. Here other aggregate interlock models will be investigated in future research projects.

ACKNOWLEDGEMENTS

Funding for this project was provided by National Science and Engineering Research Council of Canada, as well as by the Deutsche Forschungsgemeinschaft (DFG, German Research Foundation) – SFB/TRR 280. Projekt-ID: 417002380. The authors would like to thank the DFG for supporting the research project.

The work was also supported again by the Deutsche Forschungsgemeinschaft (DFG, German Research Foundation) and is part of the research project "Shear behavior of RC members without shear reinforcement—development of a consistent experimental, analytical and numerical characterization methodology" (project number 420545423, CL 789/1-1 and CH 276/9-1). This support is gratefully acknowledged.

The authors would like to thank the DFG for supporting the research project.

CONFLICT OF INTEREST

The authors declare that they have no conflicts of interest associated with the work presented in this paper.

DATA AVAILABILITY

Data on which this paper is based is available from the authors upon reasonable request.

REFERENCES

Adam, V., Schmidt, M., & Hegger, J. (2022). One-way flexural shear tests on wide reinforced concrete slab segments with simple and intermediate supports. Structural Concrete. https://doi.org/10.1002/suco.202200398

Bentz, E. C. (2005). Explaining the Riddle of Tension Stiffening Models for Shear Panel Experiments. JOURNAL OF STRUCTURAL ENGINEERING, 131(9), 1422–1425. https://doi.org/10.1061/ASCE0733-94452005131:91422

Bischoff, P. H., & Paixao, R. (2004). Tension stiffening and cracking of concrete reinforced with glass fiber reinforced polymer (GFRP) bars. Canadian Journal of Civil Engineering, 31(4), 579–588. https://doi.org/10.1139/L04-025

Classen, M. (2020). Shear Crack Propagation Theory (SCPT) – The mechanical solution to the riddle of shear in RC members without shear reinforcement. Engineering Structures, 210. https://doi.org/10.1016/j.engstruct.2020.110207

Huber, P., Huber, T., & Kollegger, J. (2016). Investigation of the shear behavior of RC beams on the basis of measured crack kinematics. Engineering Structures, 113, 41–58. https://doi.org/10.1016/j.engstruct.2016.01.025

Kani, G. N. J. (1964). The Riddle of Shear Failure and Its Solution. Journal of the American Concrete Institute, 61(4), 441–467.

KH, R. (1990). Mechanical model for the behaviour of reinforced concrete members in shear. University of Stuttgart.

KK, C., HG, P., & JK, W. (2007). Unified shear strength model for reinforced concrete beams-Part I: Development. ACI Structural Journal, 105, 142–152.

Michaluk, C. R., Rizkalla, S. H., Tadros, G., & Benmokrane, B. (1998). Flexural Behavior of One-Way Concrete Slabs Reinforced by Fiber Reinforced Plastic Reinforcements. ACI Structural Journal, 95(3), 353–364.

Oller, E., Marí, A., Bairán, J. M., & Cladera, A. (2015). Shear design of reinforced concrete beams with FRP longitudinal and transverse reinforcement. Composites Part B: Engineering, 74, 104–122. https://doi.org/10.1016/j.compositesb.2014.12.031

Reineck, K.-H. (1991). Ultimate Shear Force of Structural Concrete Members without Transverse Reinforcement Derived from a Mechanical Model. ACI Structural Journal, 88(5), 592–602.

Rombach, G. A., Kohl, M., & Nghiep, V. H. (2011). Shear design of concrete members without shear reinforcement—A solved problem? Procedia Engineering, 14, 134–140. https://doi.org/10.1016/j.proeng.2011.07.015

Schmidt, M., Schmidt, P., Wanka, S., & Classen, M. (2021). Shear response of members without shear reinforcement- experiments and analysis using shear crack propagation theory (SCPT). Applied Sciences (Switzerland), 11(7). https://doi.org/10.3390/app11073078

Tottori, S., & Wakui, H. (1993). Shear Capacity of RC and PC Beams Using FRP Reinforcement (pp. 615–632).

Wu, Y.-F., & Hu, B. (2017). Shear Strength Components in Reinforced Concrete Members. Journal of Structural Engineering, 143(9). https://doi.org/10.1061/(asce)st.1943-541x.0001832

Y, Y. (2014). Shear Behavior of Reinforced Concrete Members without Shear Reinforcement—A new Look at an old Problem. TU Delft.

Yoo, M. (2022). Experimental Study on the Shear Strength of Reinforced Concrete Beams with Various Integrated Shear Reinforcements. Materials, 15(9). https://doi.org/10.3390/ma15093091

Yost, J. R., Gross, S. P., Dinehart, D. W., & Members, A. (2001). Shear Strength Of Normal Strength Concrete Beams Reinforced With Deformed Gfrp Bars (pp. 268–275).